Spatio-temporal activity arithmetics with dopamine and acetylcholine

Introduction

1. Motivation of the occurrence of STAS
    1. ‘temporal activity sequences have been recorded from different brain regions in various tasks’ (see reference 3-11 [review 12] in Spreizer).
        1. Ref 7/8 on decision making
        2. ref 10 for learning (related to dopamine?)
1. Motivation on neuromodulator (especially dopamine)
    1. Allows for more dynamics as it can appear and disappear on different scales in time and space (reference?)
    2. Dopamine release is patchy (Patriarchi, 37)
2. Motivation on computational simulations of merging these things together
    1. feedforward networks [14] are simplest model for generating STAS [15-17]
    2. A computational model would be the Spreizer model
        1. In contrast to previous research there are no requirements on
            1. Spike frequency adaptation
            2. Spike threshold adaptation
            3. short-term synaptic depression
            4. learning rules
            5. which could also underlie the emergence of STAS (24-26)
3. Thesis: Neuromodulator such as dopamine add a layer to the network, which allows for dynamic changes of STAS

Material&Methods

Before we can introduce the additional layer to the network, we designed a model, that allows and supports the spontaneous emergence of STAS. Spreizer et al. (2019) investigated neuronal networks of ‘leaky-integrate-and-fire’ neurons. They set up local recurrent random networks (LCRN) with feedforward networks embedded in them. Moreover, a connectivity rule was used, which promotes the emergence of STAS. It introduces inhomogeneities in the spatial distribution of axons. As Spreizer et

al. pointed out, two conditions are necessary to ensure the emergence of STAS in a **EI**-network with spiking neurons: (1) each excitatory neuron projects a small fraction of their axons in a preferred direction ϕ, and (2) ϕs for neurons in the vicinity are similar, whereas ϕs are unrelated for neurons far from each other.

To consolidate the principles and arguments, under which circumstance STAS occur, we exploit a different model.

1. *The rate model (reference required)*
    1. *Advantages*
    2. *Risks*
    3. *Formulas*
    4. *Transfer function*
    5. *TAU*

In order to generate a LCRN with a wide range of possibilities, we aimed for a network with a medium number of sequences emerging. Moreover, these sequences ought have medium velocity and tend to change their direction. In the following, we specify the set of parameters to attain a network that elicit the desired properties. The study of Spreizer et al. provides an analysis of many characteristics resulting from different sets of parameter, and thus operates as an orientation for the derivation of the set of parameters. Additionally, the study provides a framework to tune the external drive with respect to various properties of the network related to STAS.

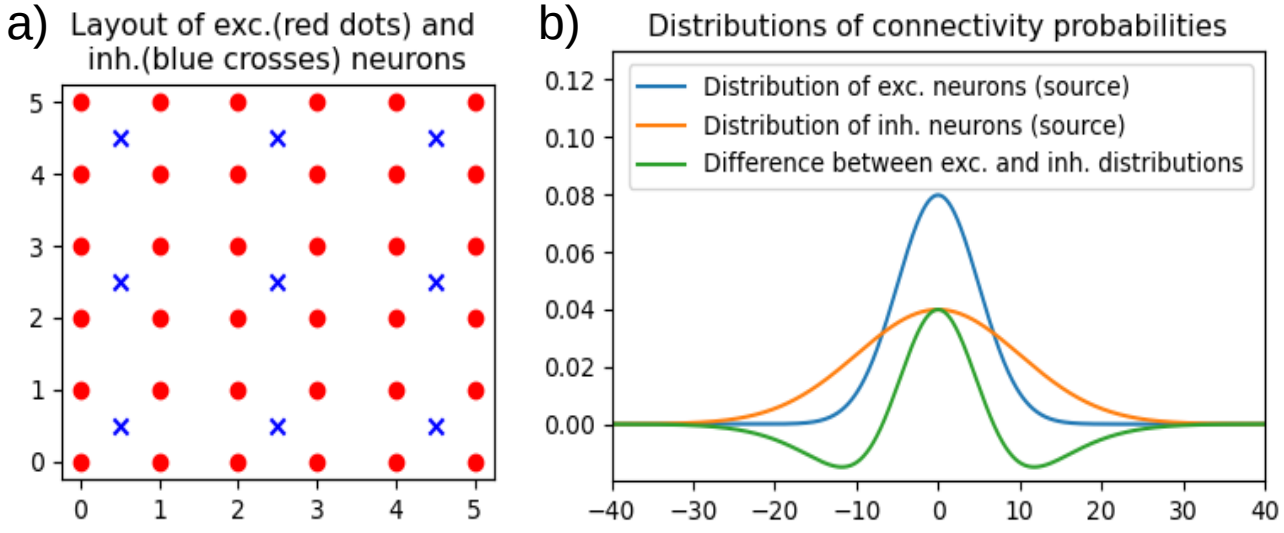

Figure 1: a) Layout of excitatory and inhibitory neurons. b) Distance-dependent connectivity probabilities of a Gaussian distribution (scaled to the grid of excitatory neurons)

Network architecture

In our study, we focus on networks with excitatory and inhibitory neurons (EI-network) commonly seen throughout various brain regions. **(reference required, relation to dopamine)**. Each neuronal

population is arranged on a square grid. The grid is folded to a torus to avoid boundary effects. [See ref. 17 of Spreizer] The excitatory neurons populate a 70x70 grid ($npop_E$ = 4900), whereas the inhibitory population ($npop_I$ = 1225) is arranged on a 35x35 grid. In contrast to Spreizer et al., we placed the inhibitory neuron as center of four excitatory neurons to ensure that each excitatory neuron has equal distance to the closest inhibitory neuron, and vice versa (Figure 1.a).

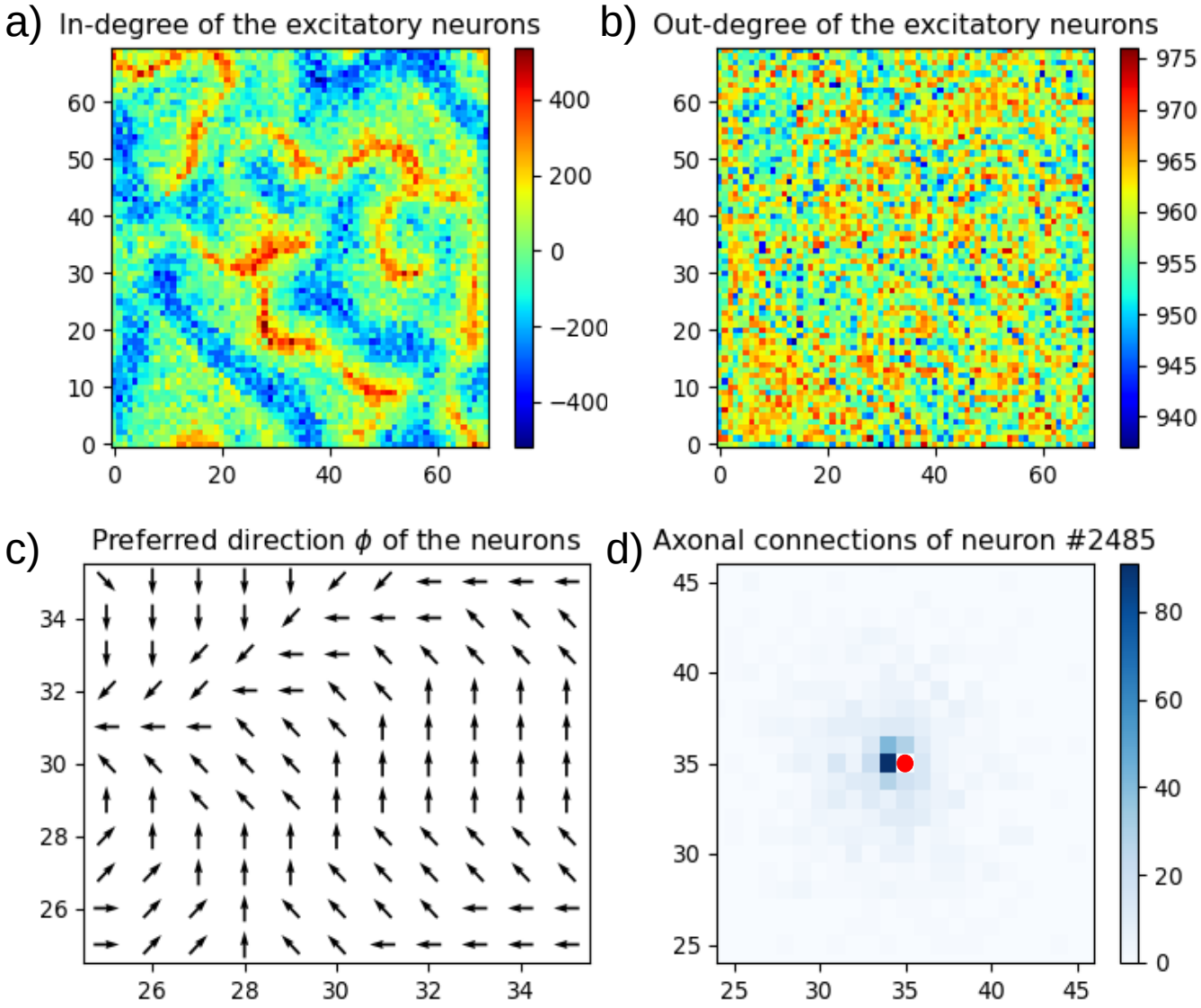

Figure 2: Network configuration: a) Shows the in-degree of the excitatory population. Inhibitory synapses are multiplied with the ratio ($npop_E$:$npop_I$ *= 4:1) and subtracted. b) the out-degree of the excitatory population is shown. c) The preferred direction ϕ is shown. According to the Perlin configuration, adjacent neurons show similar ϕs, whereas neurons far from each other are unrelated. d) The axonal directions of neuron #2485 (red dot) is shown.*

Multiple synapses to a target neuron are permitted, whereas self-connection was excluded. Therefore, each neuron forms up to 980 and 245 synapses to the excitatory and inhibitory population respectively (20% connection probability on average).

Accordingly to Spreizer et al, a distance-dependent connectivity probability is employed to determine the axonal projections. The connection probability depends on the distance between neurons and is drawn from a Gaussian distribution. The standard deviation of the Gaussian distribution, also called the space constant, is for excitatory neurons $\sigma_E = 5$, and for inhibitory neurons $\sigma_I = 5$ with respect to the correspondent grid (scaled properly for projections to the other grid) (Figure 1.b). This connectivity method tends to have a high probability of connections within the vicinity, thus they form local recurrent random networks (LCRN). ***(see Spreizer?)***

In contrast to the configuration of Spreizer et al, we used a higher average connection probability, but since the population sizes is much smaller, the total number of connections per neuron is only slightly higher. This high number of connections results in a good representation of the Gaussian distribution, such that the relative differences of synapses between adjacent target neurons is considered to be small.

Following the approach of Spreizer et al., we introduced the asymmetry of spatial connections from excitatory to excitatory neurons by the same algorithm with changes according to our different neuronal grid layout (Figure 2). The algorithm comprises the generation of Perlin noise (size: 4, base: 1), and assigns the preferred direction ϕ of the axonal direction to the neurons of the excitatory population (Figure 2.c). The synapses are shifted by one grid point in the direction ϕ. The Perlin noise and the shift are chosen such that we obtain a balance between the number of generated sequences and the tendency to change their direction. Additionally, the sequences travel with a moderate velocity (Spreizer et al., 2019). Note that the shift of synapses result in the formation of self-connections, due to the constraints, these connections were removed. The resulting network is shown in Figure 2.

The in-, and out-degree are shown only for the excitatory population. For the calculation of the in-degree, the sum of the incoming excitatory synapses **(reference for in and out-degree?)** subtracted the inhibitory synapses, corrected for the ratio between the populations ($npop_E$:$npop_I$ = 4:1) was used. The in-degree show high variations between different locations arising from the fact that the preferred direction ϕ converges in some parts – and diverges in other. In contrast, the out-degree takes only excitatory-to-excitatory synapses into account. There are neither a high variation, nor regions with high-, or low-out-degree.

The internal drive is comprised of the activity of the neurons and the synaptic weights between them. In general, the synaptic weight is $J_X = 2$, and the ***inhibition factor*** is $g = 6.5$ resulting in excitatory weights of $J_E = J_X = 2$, and $J_I = -J_X \times g = -13$. To mimic ongoing activity as input to the network, each neuron receives independent, homogeneous inputs from an external drive. This drive is modeled by a Gaussian white noise ($\mu = 25$, $\sigma = 20$). The balance of the internal and external drive was critical, and hence was carefully set with respect to the transfer function of the rate model ($x_0 = 50$, steepness = 0.5, cf. **Formula 2**)

Effect of the neuromodulator

For the simulations, we superimpose a circular patch of a neuromodulator, either DP or ACh, on the grid. The underlying neurons are affected, thus the synaptic weight of incoming synapses is increased by 20% or decreased by 25%, respectively. These values were high enough to effect the STAS, but did not lead to overexcited, nor silent regions.

Simulation parameter

Each setup is simulated for t_{sim} = 15,000 ms with a simulation resolution of 1 ms. Given the random external drive, the outcome of a long simulation does not heavily depend on the initial conditions (**reference?)**, but ensures that fundamental changes under test conditions become visible.

Before the data of the simulation is gathered, the network is given a warm-up time of t_{warm} = 500 ms. This time allowed the network to get an active state, including STAS and silent regions. In simulations with neurotransmitter patches, the warm-up was run without the effect of the neurotransmitter. Consequently, the warm-up is not considered in any analysis.

Analyses

The main focus of the analyses is on the excitatory population, because (1) the neuromodulator increases or decreases the excitability of this population, and (2) the STAS are easier to observe than in the inhibitory population.

Average activity

A simple analysis is to inspect the average activation of the neurons. Therefore, the activity of the neurons are averaged across all time points. High activation regions result from frequent activation participating in sequences and/or strong activation. Occasional active regions and/or weakly active neurons only have a small amplitude due to the long simulation time.

Effect of network changes on the average activity

The change of the synaptic weights by introducing DP or ACh is expected to influence the average activation of the neurons. In order to visualize these differences, the average activity of the baseline simulation was deducted from the average activity of the modulated network. These differences had revealed the local effect in the vicinity of the neuromodulatory patch, as well as global effects.

Number of passing sequences

Previously described analyses focus on the average activity over time, but such analyses were unable to register the number of passing sequences. Subsequently, we identified the passing sequences by an algorithm comprised of two parts: in each part, the number of threshold ($\theta = 0.25$) crossings are counted. The first part takes a subset of neurons (usually 13 neurons were used, complied with the coverage of a circle with radius r = 2), and detects the threshold crossing individually. The second part accounted for variability of the activation of the neuronal subset by averaging across neurons. Jointly, the detection gave a good estimate of the number of passing sequences, and also showed the variability of individual neurons.

Neural manifold

Sadtler et al. (2014) revealed a connection between neural manifolds and learning. Therefore, we were interested if DP can alter the neural manifold as milestone in learning a new skill or behavior. Thus, we chose the simulation data of a modulated setup, and appended it to the baseline data to achieve that the neurons are active in the same high-dimensional space. The next step was to employ a dimensional-

reduction method, namely the principal component analysis (PCA) (Cunningham and Yu 2014).The PCA analyzes a data set described by inter-correlated variables and finds a new set of orthogonal variables, called principle components (PCs), along the axes of highest variance within the data set (Jolliffe and Cadima 2016). In order to inspect the manifolds, the complete data set was projected to the first three principles.

Results

In this section, we established multiple simulations by considering different locations of modulatory patches, that might influence the characteristics of STAS. Initially, we simulated the network without any modulation, we refer to this simulation as *baseline*. By inspecting the network, we expected strong activation in regions with high in-degree (Figure 2.a). Moreover, sets of neurons sharing the same preferred direction could participate actively in STAS (not shown)**.**

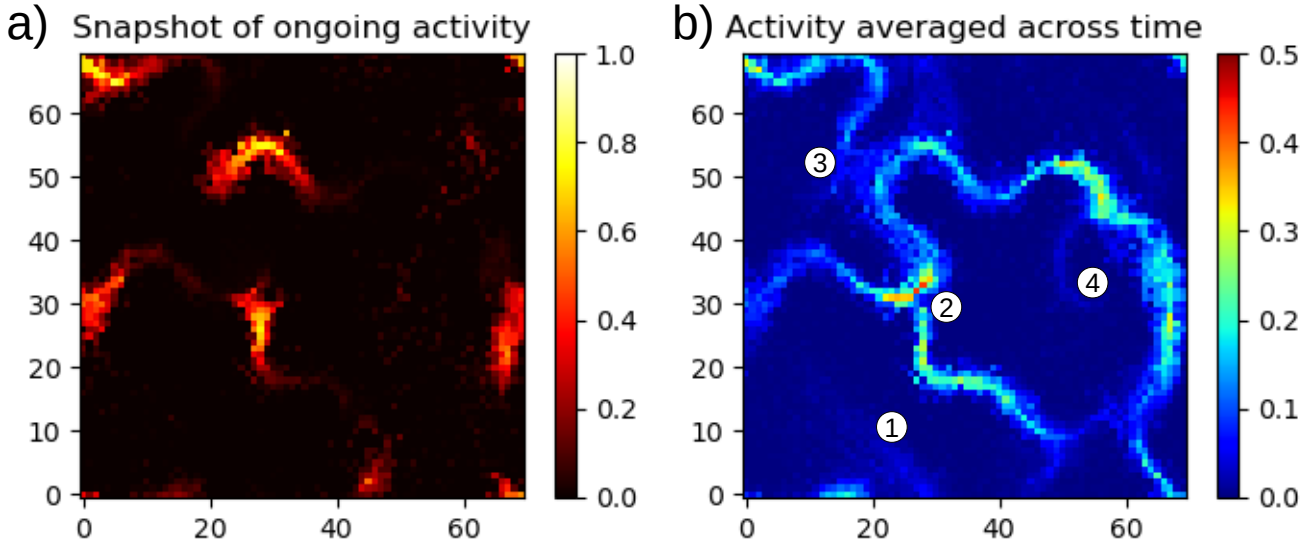

Figure 3: Baseline simulation: a) a snapshot of the ongoing activity. b) The activity averaged across time. 1-4: Locations in which different characteristics are observable. Note the different scales of graph a) and b).

In contrast to a network of spiking neurons, we can inspect the activity of neurons on a continuous scale, and not by discrete spiking events. So, we examined the activity to derive characteristics of STAS in the given network. In several locations in the network, clusters of increased activity occur, and moving across the network. We refer to these traveling clusters as STAS (Figure 3). The STAS showed strong activation in the center with decreasing activation towards the edges. Most of the STAS have a width of around six neurons, but can be broader or narrower in other locations.

STAS started and terminated in various locations. One exception might be a specific path the STAS can fare along. Since the neurons are arranged on a toroidal grid, this path can be activated in a regular fashion. Once active, a sequence can travel along the path many times. We called this the *main*. In contrast, STAS on other paths were active less often, and the STAS faded soon. We name these paths

branches (e.g 1 in Figure 3.b). At some locations, we observed converging and diverging sequences, respectively (e.g 2 and 3).

This study focused on the impact of neuromodulators on the characteristics of STAS. Therefore, we extrapolated locations, which might have the ability to change these characteristics. The first step, is to examine the effect of a modulatory patch on the STAS directly. So, we placed a patch inside, at the edge, and outside of a STAS. Secondly, a patch location was tested to increase the probability of the emergence of STAS. When the STAS got active, we employed as patch location such that the STAS did not fade quickly, especially on the main. Due to the converging and diverging character, we were interested in binary arithmetics. Specifically, we looked into patch locations to turn on or off pathways.

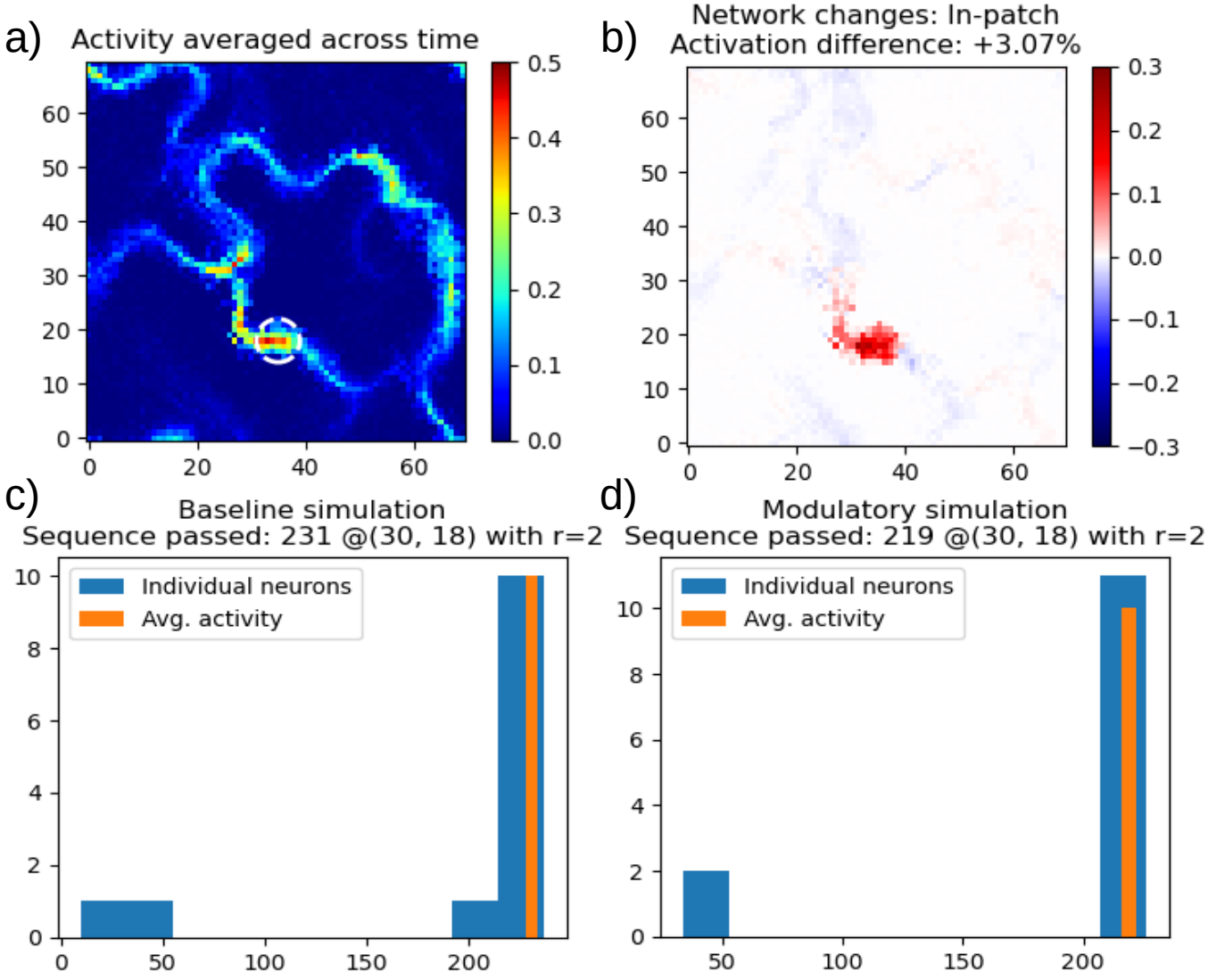

Figure 4: In-patch: a) Average activity of modulatory simulation. Dashed circle display the DP patch. b) The difference of the average activation between the modulatory and the baseline simulation. c) and d) No. of passed sequences of the baseline and the modulatory simulation, respectively.

Interestingly, we observed most STAS in regions of high in-degree, although there was one region that did not match this pattern. We investigated this region in a modulatory simulation (4 in Figure 3.b).

In-, edge-, out-patch

Initally, we investigated the effect of DP patches directly on or close to a path, but without diverging or converging branches in the vicinity. First, we placed a DP patch inside a sequence, we refer to this as in-patch simulation (Figure 4). The average activity did not show any qualitative changes of pathways STAS explore. However, the path on which the DP patch is active, increased the averaged activity at the patch, and subsequent to it. Decreased activity can be observed prior to the patch, which might result from stronger inhibition, due to a likewise more active inhibitory neurons in the patch. Moreover, the effect on the remaining network is divers. In total, the network is 3% more active.

The number of STAS was measured closely behind the patch. In the baseline and the in-patch simulation, more than 200 STAS passed the patch. Although, the number decreased with the in-patch, the overall number is still high. The small difference might be an indicator that the travel velocity of the STAS is affected by DP patches.

Secondly, the patch is moved orthogonal to the pathway to the edge of the path, we named it the edge-patch simulation.

1. Edge patch
2. Out-patch

Discussion

Open Questions

References